HHS Public Access

Author manuscript

J Am Soc Echocardiogr. Author manuscript; available in PMC 2022 August 01.

Published in final edited form as:

J Am Soc Echocardiogr. 2021 August ; 34(8): 887–895. doi:10.1016/j.echo.2021.02.018.

AUGMENTATION OF TISSUE PERFUSION WITH CONTRAST ULTRASOUND: INFLUENCE OF 3-D BEAM GEOMETRY AND CONDUCTED VASODILATION

Matthew A. Muller, B.A.[a], **Todd Belcik, B.S., A.C.S., R.D.C.S.**[a], **James Hodovan, MS, R.D.C.S.**[a], **Koya Ozawa, M.D.**[a], **Eran Brown, M.S.**[a], **Jeffry Powers, Ph.D.**[b], **Paul Sheeran, Ph.D.**[b], **Jonathan R. Lindner, M.D.**[a,c]

[a]Knight Cardiovascular Institute, Oregon Health & Science University, Portland, Oregon;

[b]Philips Ultrasound, Bothell, Washington;

[c]Oregon National Primate Research Center, Oregon Health & Science University, Portland, Oregon.

Abstract

Background: Cavitation of microbubble contrast agents with ultrasound produces shear-mediated vasodilation and an increase in tissue perfusion. We investigated the influence of the size of the cavitation volume by comparing flow augmentation produced by 2-D versus 3-D therapeutic ultrasound. We also hypothesized that cavitation could augment flow beyond the ultrasound field through release of vasodilators that are carried downstream.

Methods: In 11 rhesus macaques, cavitation of intravenously-administered lipid-shelled microbubbles was performed in the proximal forearm flexor muscles unilaterally for 10 minutes. Ultrasound cavitation (1.3 MHz, 1.5 MPa peak negative pressure) was performed with 2-D or 3-D transmission with beam elevations of 5 and 25 mm, respectively; and pulsing intervals (PI) sufficient to allow complete post-destruction refill (5 and 12 seconds for 2-D and 3-D, respectively). Contrast ultrasound perfusion imaging was performed before and after cavitation, using multiplane assessment within and beyond the cavitation field at 1.5 cm increments. Cavitation in the hindlimb of mice using 2-D ultrasound at PI of 1 or 5 seconds was performed to examine microvascular flow changes from cavitation in only arteries versus the microcirculation.

Results: In primates, the degree of muscle flow augmentation in the center of the cavitation field was similar for 2-D and 3-D conditions (5-6-fold increase for both, $p<0.01$ vs baseline). The spatial extent of flow augmentation was only modestly greater for 3-D cavitation owing to an

Address correspondence to: Jonathan R. Lindner, MD, Knight Cardiovascular Institute, UHN-62, Oregon Health & Science University, 3181 SW Sam Jackson Park Rd., Portland, OR 97239, Tel. (503) 494-3574, Fax. (503) 494-8550, lindnerj@ohsu.edu.

DISCLOSURES

Disclosures: Dr.s Powers and Sheeran are employees of Philips Ultrasound, Bothell, Washington. Their primary responsibility was to design programmed ultrasound transmission schemes on the ultrasound system.

increase in perfusion with 2-D transmission well beyond the cavitation field. In mice, cavitation in the microvascular compartment (PI 5 second) produced the greatest degree of flow augmentation, yet cavitation in the arterial compartment (PI 1 second) still produced a 3-4-fold increase in flow ($p<0.001$ vs control). Mechanism for flow augmentation beyond the cavitation zone was investigated by *in vitro* studies that demonstrated cavitation-related release of vasodilators, including ATP and nitric oxide, from erythrocytes and endothelial cells.

Conclusion: Compared with 2-D transmission, 3-D cavitation of microbubbles generates a similar degree of muscle flow augmentation, possibly because of a tradeoff between volume of cavitation and PI; and only modestly increases the spatial extent of flow augmentation because of the ability of cavitation to produce conducted effects beyond the ultrasound field.

Keywords

Cavitation; Contrast ultrasound; Microbubbles; Theranostics

Non-thermal effects of ultrasound (US) can reduce vascular tone and increase tissue perfusion.[1,2] Microstreaming and convective motion in an US field produces vasodilation of resistance arterioles through highly-conserved endothelial shear-dependent mechanisms and through the release of vasodilator substances from red blood cells (RBCs).[2–5] The vibration of conventional microbubble (MB) contrast agents in an US field, termed cavitation, increases tissue perfusion more than US alone.[4] During inertial cavitation (MB destruction), shear-mediated release of ATP occurs and secondarily acts through adenosine and production of nitric oxide (NO) and vasoactive prostanoids.[6,7] The vascular response to MB cavitation has been used to increase perfusion in the limbs of animals and humans with peripheral artery disease,[6,8] and in patients with sickle cell disease.[6] Cavitation also augments myocardial perfusion in non-human primates (NHPs),[7] serving as a potential mechanism for the reduction in infarct size recently described in patients with acute MI in whom contrast-enhanced ultrasound (CEU) cavitation was performed.[9]

Progress has been made in optimizing the acoustic output and pulse duration parameters for flow augmentation during MB cavitation.[8] It is still unknown whether broadening the US field for cavitation by using 3-D rather than 2-D array transducers will increase the amount or spatial extent of flow augmentation. If one assumes that vasodilation occurs only in vessels exposed to cavitation, then the spatial region where flow increases should monotonically increase with the tissue volume exposed to US. Yet, US-mediated flow augmentation has been observed to extend beyond the confines of the US beam.[5,6] These “conducted” effects are likely to be secondary to release of vasoactive substances into the circulation. In this study, we investigated how spatial patterns of flow augmentation are influenced by the volume of MB cavitation by comparing custom-programmed 2-D and 3-D transmission in skeletal muscle of NHPs. *In vitro* studies were performed to measure cavitation-mediated release of vasoactive substances from RBCs that could explain conducted effects beyond the limits of the US beam.

METHODS

Non-human Primate Study Design

The study was approved by the animal care and use committee at Oregon Health and Sciences University and the Oregon National Primate Research Center. Eleven adult rhesus macaques (*Mucaca mulatta*) with an average weight of 8.7±2.6 kg were studied. Animals were sedated with ketamine HCl (10 mg/kg I.M.) and anesthesia was maintained by inhaled isoflurane (1.0–2.0%) by endotracheal tube. Electrocardiography and pulse oximetry were continuously monitored, and peripheral blood pressures was recorded every 5 minutes. Low-power CEU perfusion imaging of the proximal forearm, described below, was performed bilaterally before and immediately after a 10 minute therapeutic cavitation protocol using either 2-D (n=5) or 3D (n=6) ultrasound exposure of the skeletal muscle of one forearm.

US Cavitation Therapy

Therapeutic cavitation was performed starting at the onset of an intravenous administration lipid-stabilized octafluropropane microbubble (Definity, Lantheus Medical Imaging) (1 vial diluted to 5 mL) given over 2 minutes. Ultrasound (1.3 MHz) was generated at a mechanical index of 1.3 using a 3-D matrix-array probe (X5-1) operating in either a programmed 2-D or 3-D mode (EPIQ 7, Philips Healthcare, Andover, MA). The probe was positioned 3 cm distal to the antecubital fossa with the azimuthal plane transecting the forearm in short-axis. Acoustic gel was used as an interface and the transducer was vertically positioned to place the flexor muscles at a depth of approximately 3 cm. Ultrasound was performed using 40-cycle pulse durations, and a 65-line azimuth at 1° pitch per line.[8] For 2-D exposure, a single elevational plane was generated at a pulsing interval (PI) of 5 seconds. For 3D exposure, 25 rastered elevational planes were generated using a PI of 12 seconds per exposure. The longer PI for 3D conditions was based on experiments using a second imaging probe for CEU perfusion assessment to measure the time necessary for 3D volume refill after a therapeutic cavitation pulse. The total duration of cavitation was 10 minutes.

Acoustic Field Testing

Acoustic pressures generated by the X5-1 transducer were measured spatially (see Online Supplemental Methods).

Non-Human Primate Perfusion Imaging

CEU perfusion imaging (Sequoia 512, Siemens Medical, Mountain View, California) with a linear-array transducer was performed using contrast-specific phase-inversion and amplitude-modulation at 7 MHz and a mechanical index (MI) of 0.18. A vial of Definity was diluted to a total volume of 15 mL with saline and infused at 1 ml/min. Perfusion imaging was performed bilaterally before and immediately after cavitation imaging. The imaging transducer was positioned to image the short-axis plane that represented the geometric center of the therapeutic transducer, referred to as level 0 (L_0). For the post-therapy stage, perfusion imaging in the cavitation-exposed limb was performed with additional short-axis planes at 1.5 cm proximal to L_0 ($L_{-1.5}$) and at three sites at 1.5 cm increments beyond L_0 ($L_{1.5}$, $L_{3.0}$, and $L_{4.5}$). CEU images were analyzed (Narnar LLC, Portland, OR) by measuring

background-subtracted intensity from the forearm digital-flexor muscle group and fitting data to: $y=A(1-e^{-\beta t})$ where y is acoustic intensity at time t, A is the plateau intensity reflecting relative blood volume, and the rate constant β represents microvascular flux rate.[10] Muscle blood flow was calculated as the product of A and β. Noncapillary microvascular blood volume (NCMBV), an index of arterial and arteriolar vasodilation, was measured by a refitted time-intensity curve that used a PI of 2 seconds as background, and subtracting the resulting A-value from the initial A-value, thereby eliminating most capillary signal.[11]

Murine Experiments

Cavitation-mediated flow augmentation in the hindlimb of C57Bl/6 mice was used as a complimentary model for investigating downstream conducted vasodilation. Mice were anesthetized with isoflurane and a jugular vein was cannulated for administration of microbubbles. A 2-D phased-array US transducer (Sonos 7500, Philips Ultrasound, Andover, MA) was positioned to image the proximal hindlimb transaxially using power harmonic Doppler mode at 1.3 MHz, a mechanical index of 1.3, and a pulse-repetition frequency of 9300 Hz. Lipid-shelled decafluorobutane microbubbles were prepared.[6] Microbubbles (2×10^8) were administered as an intravenous bolus. Cavitation was performed using one of the following conditions: (a) PI of 5 seconds for 10 minutes (n=9), (b) PI of 1 second for 2 minutes (n=11), or (iii) PI of 1 second for 10 minutes (n=14). These conditions were selected on the basis of curve modeling and visually observing time-intensity data during CEU of the hindlimb (see Results) in order to achieve cavitation in either high-velocity intra-muscular arteries (PI 1 second) versus in the distal downstream microcirculation (PI 5 seconds). The two different total durations for cavitation at PI=1 were intended to match conditions at a PI of 5 seconds in terms of either the number of frames (n=120 over 2 minutes) or duration of exposure (10 minutes). Muscle perfusion was assessed using CEU imaging protocols identical to those above, and a MB infusion rate of 2×10^5 min^{-1}.

Ex Vivo Arterial Dilation

To determine the importance of RBCs as a source for vasodilators during conducted arterial dilation, *ex vivo* arterial dilation studies were performed in perfused rat mesenteric arteries with or without RBCs, and with and without MB cavitation (see Supplemental Methods).

In vitro Erythrocyte ATP and NO Release

Release of the vasoactive mediators ATP and NO from RBCs during cavitation was assessed using a luciferin-luciferase assay for ATP, and an amperometric electrochemical sensing probes for NO (see Supplemental Methods).

Statistical Analysis

Data were analyzed using Prism (version 8.4, GraphPad, San Diego, CA). For data determined to be non-normally distributed by the D'Agostino and Pearson omnibus test, group-wise differences were assessed by Mann-Whitney U test for non-paired data or Wilcoxon signed-rank test for paired data. Non-normally distributed data are displayed graphically as box-whisker plots illustrated median (*bar*), interquartile range (*box*), and

range (*whiskers*); and numerically as median and 95% confidence intervals (CI). For normally-distributed data, group-wise differences were assessed by paired or unpaired Student's t-test. For NHP studies, multiple comparisons were made using a Kruskal-Wallis or Friedman's test with post-hoc Dunn's correction for multiple comparisons. Differences were considered significant at $p<0.05$.

RESULTS

Flow Augmentation with 2D and 3D Cavitation Fields

Calibrated hydrophone measurements were made when operating the X5-1 matrix-array transducer in the programmed 2-D (1-sector) or 3-D (25-sector) transmission schemes. The beam elevational dimension 3 cm distance from the transducer face, representing mid-muscle depth for NHP experiments, was approximately 5 mm during 2-D cavitation and 25 mm during 3-D cavitation (Figure 1). Using the programmed outputs for *in vivo* cavitation, the peak negative acoustic pressure at the focus was 1.5 MPa.

Bilateral forearm skeletal muscle CEU perfusion imaging was performed before and after ten minutes of unilateral therapeutic cavitation. In the therapy arm, CEU was performed at 1.5 cm increments proximal and distal to the estimated mid-elevation plane during cavitation (Figure 2A). In the center position (L_0), the degree to which flow was augmented was similar (5-6-fold increase) for 2-D and 3-D cavitation conditions (Figure 2B and 2C). Similar degree of flow augmentation in the center of the cavitation volume (L_0-plane) occurred despite having 2.4-fold greater number of cavitation events for 2-D versus 3-D, based on differences in PI required for MB replenishment. Flow increased only modestly in the contralateral control arm, though these changes did not meet statistical significance. When evaluating the spatial distribution of post-cavitation flow along the forearm, there were only subtle differences between 2-D and 3-D cavitation conditions (Figure 2D to 2F). Flow augmentation at $L_{1.5}$, located at the distal margin of the 3-D cavitation field but well beyond the margin of the 2-D field, was greater for 3-D than 2-D cavitation, although this difference did not reach statistical significance (median: 14.8 [95% C.I. 7.1–31.4] vs. 6.5 [95% C.I. 1.5–17.6] IU/s, $p=0.12$). On parametric analysis, flow augmentation was attributable to somewhat greater increases in microvascular blood volume than microvascular flux rate (Supplemental Figure 1). The NCMBV was calculated by modeling time-intensity data and served as an indicator of dilation of intramuscular small arteries and arterioles. The degree of vasodilation by NCMBV was similar between 2-D and 3D cavitation conditions (Figure 3), with the exception that 3-D cavitation resulted in a higher NCMBV at the most distal plane of $L_{4.5}$ (median: 11.2 [95% C.I. 6.0 to 16.0] vs. 4.8 [95% C.I. 2.5 to 11.5] IU, $p=0.01$). There were no significant differences in vital signs when comparing NHPs assigned to 2D versus 3D cavitation, nor were there any significant changes during high-MI cavitation (Table 1).

Cavitation in Macrovascular and Microvascular Compartments

The NHP experiments indicated that vasodilation and flow augmentation occur beyond the confines of the cavitation volume. To investigate the downstream delivery of vasodilators, flow augmentation in the hindlimb of mice was compared using conditions designed to

cavitate MBs in either the arterial compartment, or in both the arterial and microvascular compartments. Time-intensity data from CEU and videos with maximum-intensity projection indicated that at PI of 1 second cavitation in the hindlimb adductor occurs primarily in high-velocity intramuscular arteries (Figure 4A and 4B, Supplemental Videos). At a PI of 5 seconds, cavitation occurs in both arteries and the downstream microcirculation. The degree to which muscle flow was augmented was greatest after cavitation at a PI of 5 seconds (Figure 4C). Yet, substantial augmentation in perfusion was also seen at a PI of 1 second whether matching to PI=5 seconds was made in terms of the number of frames (2 minute protocol) or the duration of cavitation (10 minute protocol).

Contribution of RBCs to Cavitation Therapy

Because conducted vasodilation beyond the US volume is likely to involve cavitation-mediated release of vasoactive compounds, including those that are released by RBCs, we evaluated *ex vivo* arterial responses when cavitation was performed with an acellular versus RBC-perfused system (Figure 5A and 5B). The addition of RBCs to the perfusate but without cavitation decreased arterial resistance, an effect that is known to occur from an increase shear stress vis-a-vis viscosity, and vasodilator release from RBCs in vascular shear.[12] Ultrasound cavitation decreased arterial resistance irrespective of whether or not the perfusate contained RBCs. The combination of RBCs and cavitation of MBs produced the greatest drop in arterial resistance.

Release of ATP and NO from RBCs During Cavitation.

Cavitation using similar acoustic conditions in this study has already been shown to trigger the sustained release ATP from endothelial cells and to increase tissue NO concentration.[6] We investigated whether RBCs also serve as a source for vasodilator release with brief cavitation. Optical imaging studies detected a large and immediate release of ATP from RBCs in vitro after cavitation (Figure 5C). Signal for ATP declined rapidly over 20 minutes, which likely reflected exhaustion of substrate for the luciferin-luciferase assay. On real-time electrochemical sensing, the onset of cavitation produced NO release from RBCs in whole blood which accumulated over the 1 minute period of US exposure, and stabilized after US was discontinued (Figure 5E). The average increase in NO concentration during cavitation was approximately 200 nM, which is within the physiologic range for NO-mediated vasodilation, whereas release was not detected for control experiments (Supplemental Figure 2).

DISCUSSION

A variety of biologic effects occur in cells that are adjacent to MB inertial cavitation events.[6,13,14] These effects have been leveraged for theranostic US applications for cardiovascular disease including focal gene or drug delivery, thrombolysis, or augmentation in tissue perfusion.[6,7,9,15,16] All of these applications are influenced by the US parameters that govern how cavitation influences surrounding cells.

Inertial cavitation of MBs at frequencies and acoustic pressures that are within the conventional diagnostic range have been shown to augment perfusion in the myocardium

and limb skeletal muscle in small and large animal models, and in humans.[4,6–8] Mechanistic studies indicate that vascular conductance increases secondary to a complex network of events that occur from high shear produced at the site of intravascular MB cavitation. These events include shear-dependent NO release; and focal release of ATP from microporation and sustained ATP channel activation with subsequent purinergic signaling through ATP and adenosine receptors on and downstream production of NO and vasoactive prostaglandins.[4,6,7] Optimal acoustic conditions for these events have been studied. Not surprisingly, flow augmentation is most effective when MB doses are high, US power is sufficient to produce inertial cavitation, and US pulse duration is long which produces sustained cavitation.[4,8] Using these parameters, it has been possible to increase flow by several fold in the limbs of patients with peripheral artery disease and sickle cell disease.[6,8]

For many of the therapeutic applications of CEU, it is desirable to produce a focal region of US exposure for site-targeted therapy. An exception is when cavitation is used to treat ischemia that involves an entire limb or coronary artery territory. The overall aim of this study was to investigate how the volume of tissue exposed to cavitation influences either the degree or spatial extent of flow augmentation. We compared 2-D and 3-D cavitation conditions using a matrix array transducer programmed to produce optimized pulses with regard to azimuthal line density and number of cycles.[8] When considering cavitation volumes, the term “2-D” is imprecise since it refers to the volume-averaged display generated by a single beam sweep. In other words, 2-D imaging occurs in a “slab” of tissue that, in this study, had an elevational thickness of 5 millimeters. In comparison, 3-D imaging used 25 rastered sweeps at a programmed pitch of 1.5° to yield a total effective thickness of around 25 mm.

It would have been reasonable to expect 3-D cavitation to produce more flow augmentation than 2-D based on a greater volume of tissue where vasodilation occurs, thereby lowering resistance in a large portion of the vascular network. Yet, compared to 2-D cavitation, 3-D cavitation did not substantially increase the degree of flow in the center of the volume (L_0). This finding was not entirely unexpected since a larger beam volume must be offset by a reduced periodicity of volumetric transmits needed to allow replenishment of the microcirculation with non-cavitated MBs. We were able to achieve a degree of flow augmentation in the center of the cavitation field (L_0) that was about half that which occurs with moderate contractile exercise of the forearm in NHPs.[17]

With respect to the spatial extent of flow augmentation, 3-D cavitation resulted in only modest advantages to 2D in the spatial extent of flow augmentation and vasodilation (NCMBV) in regions at the margins of the 3-D US field. The primary reason for the finding that 3-D was only modestly advantageous in its spatial effects was that flow augmentation occurred well outside the US field for 2-D cavitation conditions. This phenomenon has been observed previously in mice undergoing MB cavitation of the hindlimb.[6] When using intravascular US catheters without MBs, US generated focally in arteries can produce flow augmentation far downstream.[5] In these studies, the spacing between US and flow augmentation is out of proportion to what one would expect from channel-mediated (e.g. connexin) cell-cell signaling of shear-events.[18] Instead conducted effects are more likely from systemic release of NO, ATP, and possibly other shear-dependent compounds from

endothelial cells and RBCs.[5,6] Murine experiments in the current study using different PIs to control the vascular compartment where cavitation occurs further supported the concept that flow can be conducted downstream from cavitation events. Conducted effects could also explain why the plane that appeared to benefit the most benefit from 3-D exposure was $L_{1.5}$, a location that would be affected both by MB cavitation within the microcirculation and by conducted effects from several upstream planes.

The *ex vivo* artery experiments in the current study supported the idea that vasodilator release from both endothelial cells and RBCs contribute to vasodilation. Effects of US alone and MB cavitation on endothelial-dependent vasodilator response have been well characterized.[3,4,6,19,20] The contribution of RBCs to US-mediated vasodilation has recently become recognized.[5,6] In the current study, brief cavitation of MBs mixed with RBCs triggered the immediate release of ATP. This finding is not unexpected given high erythrocyte ATP concentrations and presence of ATP channels, such as pannexins, on erythrocytes.[21] We also demonstrated, for the first time, that MB cavitation can trigger the release of NO from RBCs in whole blood. Shear-dependent release of RBC-derived NO, which binds reversibly in the form of s-nitrosylhemoglobin, is a conserved mechanism by which RBCs can influence regional vascular tone.[21,22] The increase in NO concentration that was detected, around 200 nM, is within or even beyond the physiologic range needed for vasodilation in vivo.[23] These systemically-released factors serve as an explanation for the increases in flow seen also in the contralateral limb. However, changes in perfusion in the contralateral limb were small compared to those tissues nourished by arterial beds immediately downstream in the cavitation-exposed arm, as would be expected through processes of both hemodilution and metabolism of vasodilators.

There are several clinical implications of this study. Three-dimensional cavitation conditions are probably warranted to augment flow in tissues that are hypoperfused and when the location of the targeted microcirculation is discrete and predictable. An important consideration for myocardial flow augmentation is that 3-D cavitation exposes not only the muscle microcirculation but also the LV cavity. This exposure could further promote flow augmentation by releasing vasodilators in a large amount of blood volume just upstream from the coronary arteries, but could also be detrimental by eliminating MBs from the blood pool and preventing coronary microvascular cavitation. Accordingly, whether using cavitation to augment flow or to enhance thrombolysis, pulsing intervals would have to be carefully optimized for 3-D exposure. For the sonothrombolysis application, selection of the optimal approach (2-D or 3-D) will rely on further mechanistic understanding of whether lysis should be targeted at coronary artery recanalization or re-opening of the distal microcirculation.[9,24] For limb flow augmentation, it is likely that conducted vasodilation would be advantageous based on the total size of the 3-D transducers and the probability that MB concentration in the microcirculation of the ischemic distal limb will be extremely low based on tissue blood flows of <0.05 ml/min/g tissue.

There are limitations of this study that require mention. Firstly, our small NHP sample sizes could have led to an underestimation of statistical differences between 2-D and 3-D cavitation. The larger volume of cavitation with 3-D imaging required a reduction in the PI to allow complete refill. It is likely that there were approximately the same number of MB

cavitation events for 2-D (more frequent events in a smaller volume) and 3-D imaging (less frequent events in a larger volume). Because we were investigating local and systemic effects, we were able to perform cavitation only on one forearm per setting. We also did not examine the effect of cavitation farther down the forearm in NHPs. The relative importance of RBCs versus the endothelium, or ATP versus NO for flow augmentation was not investigated, but also was not the primary focus of the current study.

In summary, compared with 2-D conditions, 3-D cavitation of microbubbles generates a similar degree of muscle flow augmentation, possibly because of a tradeoff between volume of cavitation and PI. Large volume 3-D cavitation increases the spatial extent of flow augmentation. Yet this benefit is modest because of the ability of inertial cavitation to produce conducted effects beyond the ultrasound field. These findings are likely to influence future planning of studies of cavitation-mediated bioeffects that may involve not only local but also conducted effects from upstream events.

Supplementary Material

Refer to Web version on PubMed Central for supplementary material.

FUNDING

Dr. Lindner is supported by grants R01-HL078610, R01-HL130046, and P51-OD011092 from the National Institutes of Health (NIH); and by grant 18-18HCFBP_2-0009 from NASA. Dr. Ozawa is supported by the JSPS Overseas Research Fellowship and Manpei Suzuki Diabetes Foundation. Mr. Brown was supported by a pre-doctoral grant 18PRE33960532 from the American Heart Association.

ABBREVIATIONS

ATP	adenosine triphosphate
CEU	contrast-enhanced ultrasound
MB	microbubbles
MI	mechanical index
NCMBV	non-capillary microvascular blood volume
NO	nitric oxide
PI	pulsing interval
RBC	red blood cell

REFERENCES

[1]. Iida K, Luo H, Hagisawa K, Akima T, Shah PK, Naqvi TZ, et al. Noninvasive low-frequency ultrasound energy causes vasodilation in humans. J Am Coll Cardiol. 2006;48:532–7. [PubMed: 16875980]

[2]. Siegel RJ, Suchkova VN, Miyamoto T, Luo H, Baggs RB, Neuman Y, et al. Ultrasound energy improves myocardial perfusion in the presence of coronary occlusion. J Am Coll Cardiol. 2004;44:1454–8. [PubMed: 15464327]

[3]. Suchkova VN, Baggs RB, Sahni SK, Francis CW. Ultrasound improves tissue perfusion in ischemic tissue through a nitric oxide dependent mechanism. Thromb Haemost. 2002;88:865–70. [PubMed: 12428107]

[4]. Belcik JT, Mott BH, Xie A, Zhao Y, Kim S, Lindner NJ, et al. Augmentation of limb perfusion and reversal of tissue ischemia produced by ultrasound-mediated microbubble cavitation. Circ Cardiovasc Imaging. 2015;8:e002979. [PubMed: 25834183]

[5]. Muller MA, Xie A, Qi Y, Zhao Y, Ozawa K, Noble-Vranish M, et al. Regional and Conducted Vascular Effects of Endovascular Ultrasound Catheters. Ultrasound Med Biol. 2020;46:2361–9. [PubMed: 32522456]

[6]. Belcik JT, Davidson BP, Xie A, Wu MD, Yadava M, Qi Y, et al. Augmentation of Muscle Blood Flow by Ultrasound Cavitation Is Mediated by ATP and Purinergic Signaling. Circulation. 2017;135:1240–52. [PubMed: 28174191]

[7]. Moccetti F, Belcik T, Latifi Y, Xie A, Ozawa K, Brown E, et al. Flow Augmentation in the Myocardium by Ultrasound Cavitation of Microbubbles: Role of Shear-Mediated Purinergic Signaling. J Am Soc Echocardiogr. 2020;33:1023–31 e2. [PubMed: 32532642]

[8]. Mason OR, Davidson BP, Sheeran P, Muller M, Hodovan JM, Sutton J, et al. Augmentation of Tissue Perfusion in Patients With Peripheral Artery Disease Using Microbubble Cavitation. JACC Cardiovasc Imaging. 2020;13:641–51. [PubMed: 31422129]

[9]. Mathias W Jr., Tsutsui JM, Tavares BG, Fava AM, Aguiar MOD, Borges BC, et al. Sonothrombolysis in ST-Segment Elevation Myocardial Infarction Treated With Primary Percutaneous Coronary Intervention. J Am Coll Cardiol. 2019;73:2832–42. [PubMed: 30894317]

[10]. Wei K, Jayaweera AR, Firoozan S, Linka A, Skyba DM, Kaul S. Quantification of myocardial blood flow with ultrasound-induced destruction of microbubbles administered as a constant venous infusion. Circulation. 1998;97:473–83. [PubMed: 9490243]

[11]. Pascotto M, Leong-Poi H, Kaufmann B, Allrogen A, Charalampidis D, Kerut EK, et al. Assessment of ischemia-induced microvascular remodeling using contrast-enhanced ultrasound vascular anatomic mapping. J Am Soc Echocardiogr. 2007;20:1100–8. [PubMed: 17566703]

[12]. Richardson KJ, Kuck L, Simmonds MJ. Beyond oxygen transport: active role of erythrocytes in the regulation of blood flow. Am J Physiol Heart Circ Physiol. 2020;319:H866–H72. [PubMed: 32857630]

[13]. Meijering BD, Juffermans LJ, van Wamel A, Henning RH, Zuhorn IS, Emmer M, et al. Ultrasound and microbubble-targeted delivery of macromolecules is regulated by induction of endocytosis and pore formation. Circ Res. 2009;104:679–87. [PubMed: 19168443]

[14]. Wu J, Nyborg WL. Ultrasound, cavitation bubbles and their interaction with cells. Adv Drug Deliv Rev. 2008;60:1103–16. [PubMed: 18468716]

[15]. Unger E, Porter T, Lindner J, Grayburn P. Cardiovascular drug delivery with ultrasound and microbubbles. Adv Drug Deliv Rev. 2014;72:110–26. [PubMed: 24524934]

[16]. Kuliszewski MA, Kobulnik J, Lindner JR, Stewart DJ, Leong-Poi H. Vascular gene transfer of SDF-1 promotes endothelial progenitor cell engraftment and enhances angiogenesis in ischemic muscle. Mol Ther. 2011;19:895–902. [PubMed: 21364544]

[17]. Chadderdon SM, Belcik JT, Smith E, Pranger L, Kievit P, Grove KL, et al. Activity restriction, impaired capillary function, and the development of insulin resistance in lean primates. Am J Physiol Endocrinol Metab. 2012;303:E607–13. [PubMed: 22739105]

[18]. Bagher P, Segal SS. Regulation of blood flow in the microcirculation: role of conducted vasodilation. Acta Physiol (Oxf). 2011;202:271–84. [PubMed: 21199397]

[19]. Sugita Y, Mizuno S, Nakayama N, Iwaki T, Murakami E, Wang Z, et al. Nitric oxide generation directly responds to ultrasound exposure. Ultrasound Med Biol. 2008;34:487–93. [PubMed: 17933454]

[20]. Maruo A, Hamner CE, Rodrigues AJ, Higami T, Greenleaf JF, Schaff HV. Nitric oxide and prostacyclin in ultrasonic vasodilatation of the canine internal mammary artery. Ann Thorac Surg. 2004;77:126–32. [PubMed: 14726048]

[21]. Sridharan M, Adderley SP, Bowles EA, Egan TM, Stephenson AH, Ellsworth ML, et al. Pannexin 1 is the conduit for low oxygen tension-induced ATP release from human erythrocytes. Am J Physiol Heart Circ Physiol. 2010;299:H1146–52. [PubMed: 20622111]

[22]. Allen BW, Stamler JS, Piantadosi CA. Hemoglobin, nitric oxide and molecular mechanisms of hypoxic vasodilation. Trends Mol Med. 2009;15:452–60. [PubMed: 19781996]

[23]. Bohlen HG. Is the real in vivo nitric oxide concentration pico or nano molar? Influence of electrode size on unstirred layers and NO consumption. Microcirculation. 2013;20:30–41. [PubMed: 22925222]

[24]. Lindner JR. Therapeutic Contrast Echocardiography: Bubbles Become Medicine. J Am Coll Cardiol. 2019;73:2843–5. [PubMed: 31171089]

HIGHLIGHTS

- Ultrasound cavitation can increase tissue blood flow through shear effects;
- 3-D vs 2D cavitation modestly increases the degree and spatial extent of flow augmentation
- Cavitation causes release of vasodilators from endothelium and RBCs that are conducted downstream.

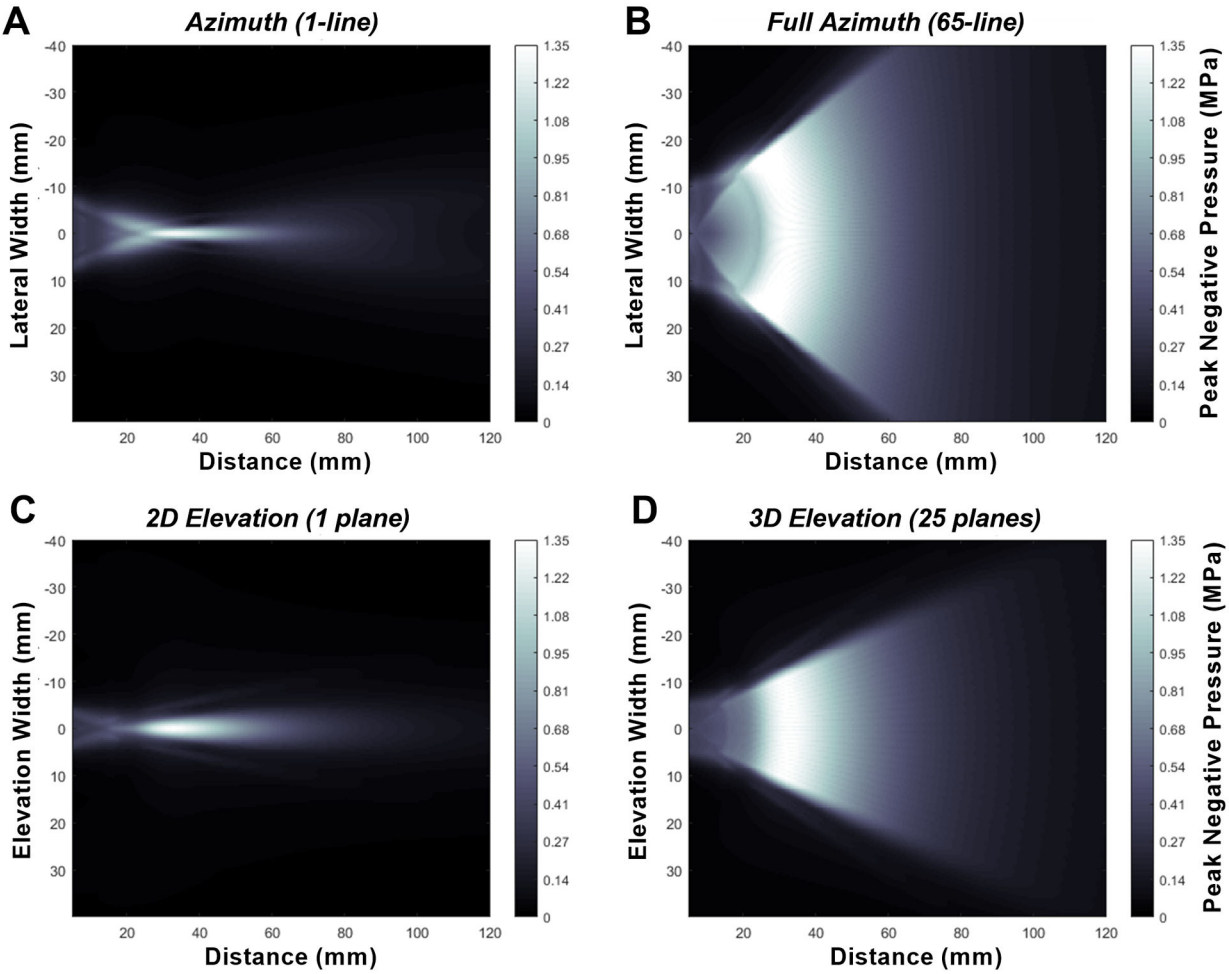

Figure 1.

Visual display of ultrasound peak negative acoustic pressure with increasing distance (*x-axis*) from the ultrasound probe. For y-axis, dimensions are shown for (**A**) a single ultrasound line in the azimuthal dimension, (**B**) the full 65-line azimuthal profile, (**C**) the elevational dimension for the 2-D (1 elevational plane) transmission, and (**D**) the elevational dimension for the 3-D (25 elevational plane) transmission.

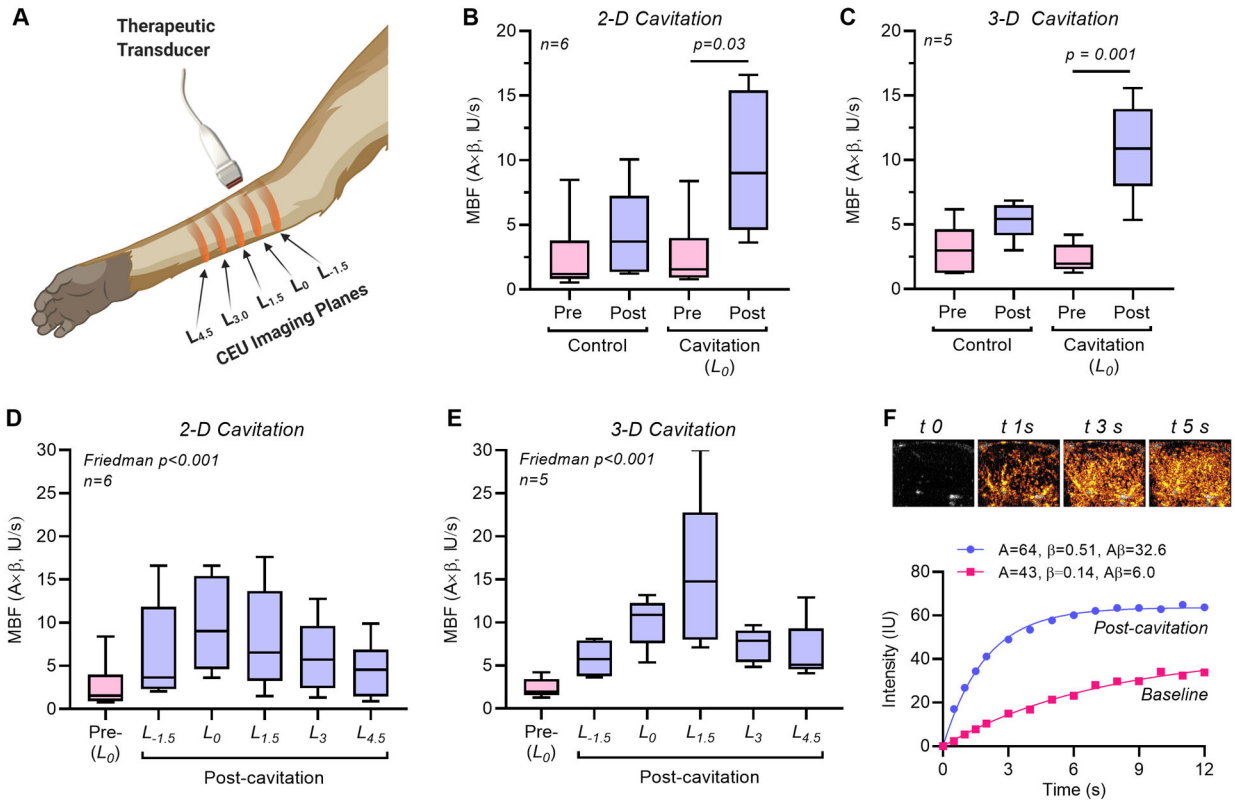

Figure 2.

Influence of 2-D versus 3-D cavitation on forearm perfusion in rhesus macaques. (**A**) Illustration of the CEU perfusion imaging planes in the post-treatment arm that were classified as being at the center of cavitation field (L_0) or at 1.5 cm increments proximal or distal to the center. (**B, C**) Microvascular blood flow (*MBF*) in the control and cavitation-treated arm (central L_0 plane) at baseline and after 10 minutes of cavitation with 2-D or 3-D transmission. (**D, E**) Microvascular blood flow (*MBF*) in the cavitation-treated arm at baseline (L_0 plane) and after cavitation (all planes) after 10 minutes of cavitation with 2-D or 3-D transmission. (**F**) Example of post-destruction time-intensity-curves on CEU perfusion imaging at the L_0 plane at baseline and after 3-D cavitation, and source data of background-subtracted CEU images at select time intervals in seconds (t_x) post-cavitation illustrating a 5-6-fold increase in perfusion (Aβ).

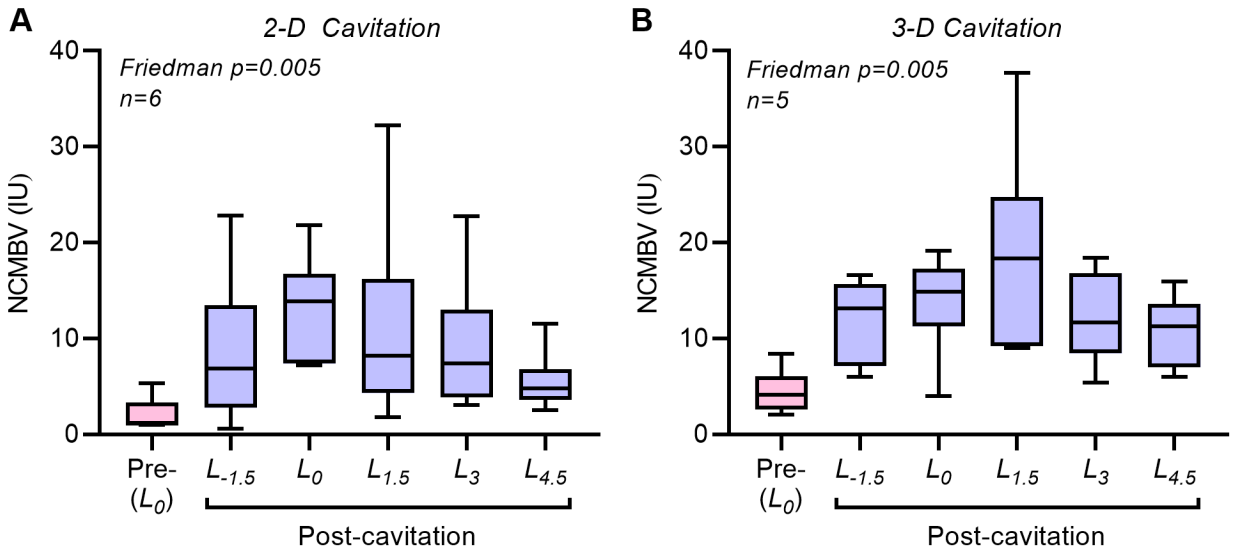

Figure 3.

Non-capillary microvascular blood flow (*MCMBV*), an index of the degree of arterial and arteriolar vasodilation, in the cavitation-treated arm at baseline (L_0 plane) and after cavitation (all planes) after 10 minutes of cavitation with (**A**) 2-D or (**B**) 3-D transmission.

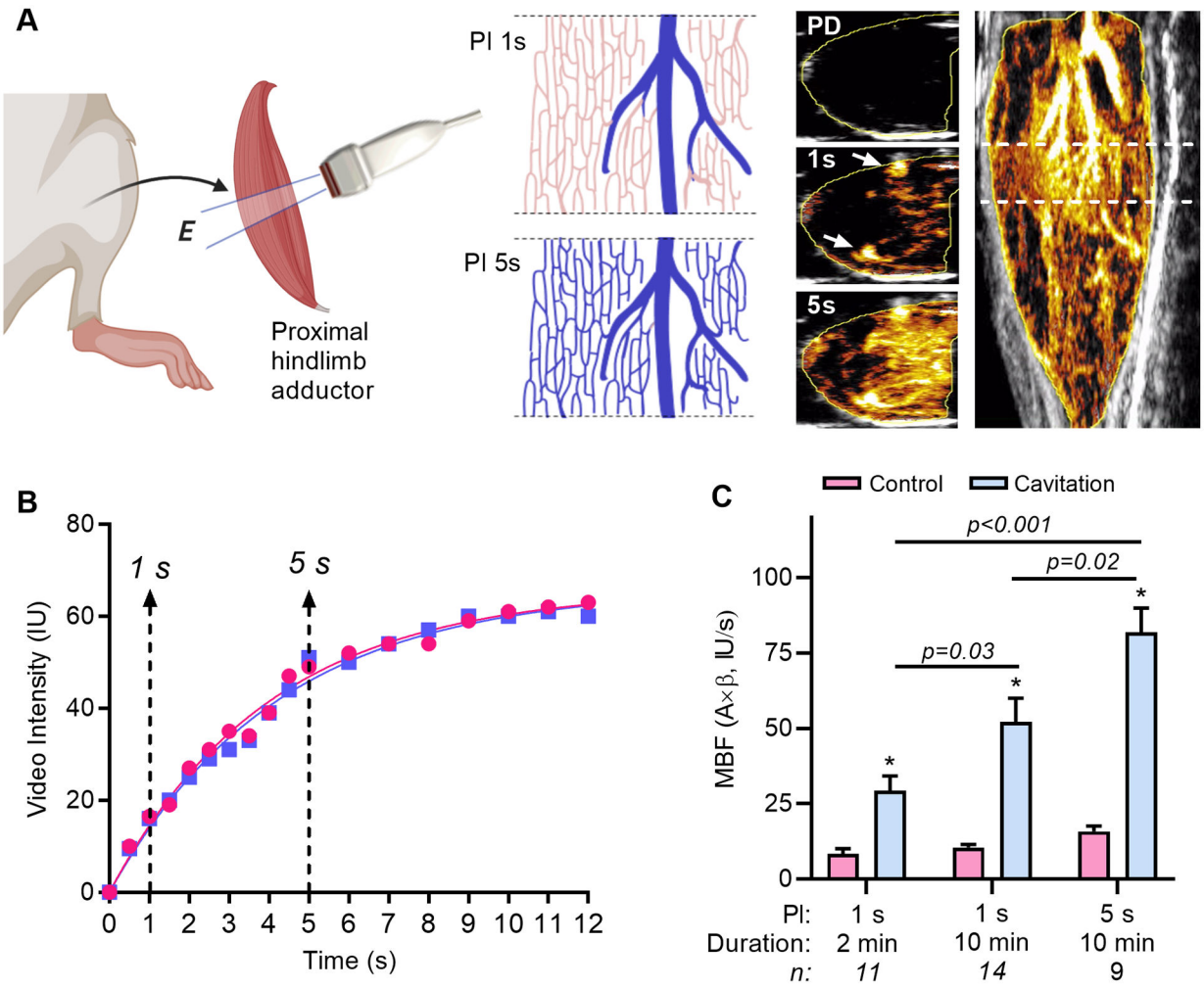

Figure 4.

The modification of cavitation pulsing interval (PI) in mice to investigate conducted vasodilation. (**A**) Short-axis cavitation was performed in the proximal hindlimb adductor muscle with 2-D transmission (*E*, elevational plane). Shown in the schematic, vascular refill with microbubles within the elevation between cavitation frames (*blue*) occurs only in large intramuscular vessels with fast velocity at a pulsing interval (*PI*) of 1 second, and in most of the slow velocity microcirculation at 5 seconds. This paradigm was verified by examining CEU perfusion imaging data with maximum intensity projection where transaxial imaging from the plane shown by the dashed lines on the long-axis image (far right) showed no microbubble enhancement immediately post-destruction (*PD*), enhancement primarily of large arteries at 1 second (arrows), and microvascular enhancement at 5 seconds (see corresponding on-line videos). (**B**) Two separate post-destruction time-intensity curves during CEU imaging obtained 1 min apart illustrating only partial microbubble refill (arterial) at 1 second, and near complete refill (arterial and microcirculation) at 5 seconds. (**C**) Mean (±SEM) microvascular blood flow (*MBF*) in the cavitation-exposed and contralateral control limb after 10 min of therapy using a PI of 1 second or 5 seconds. *p<0.001 versus control.

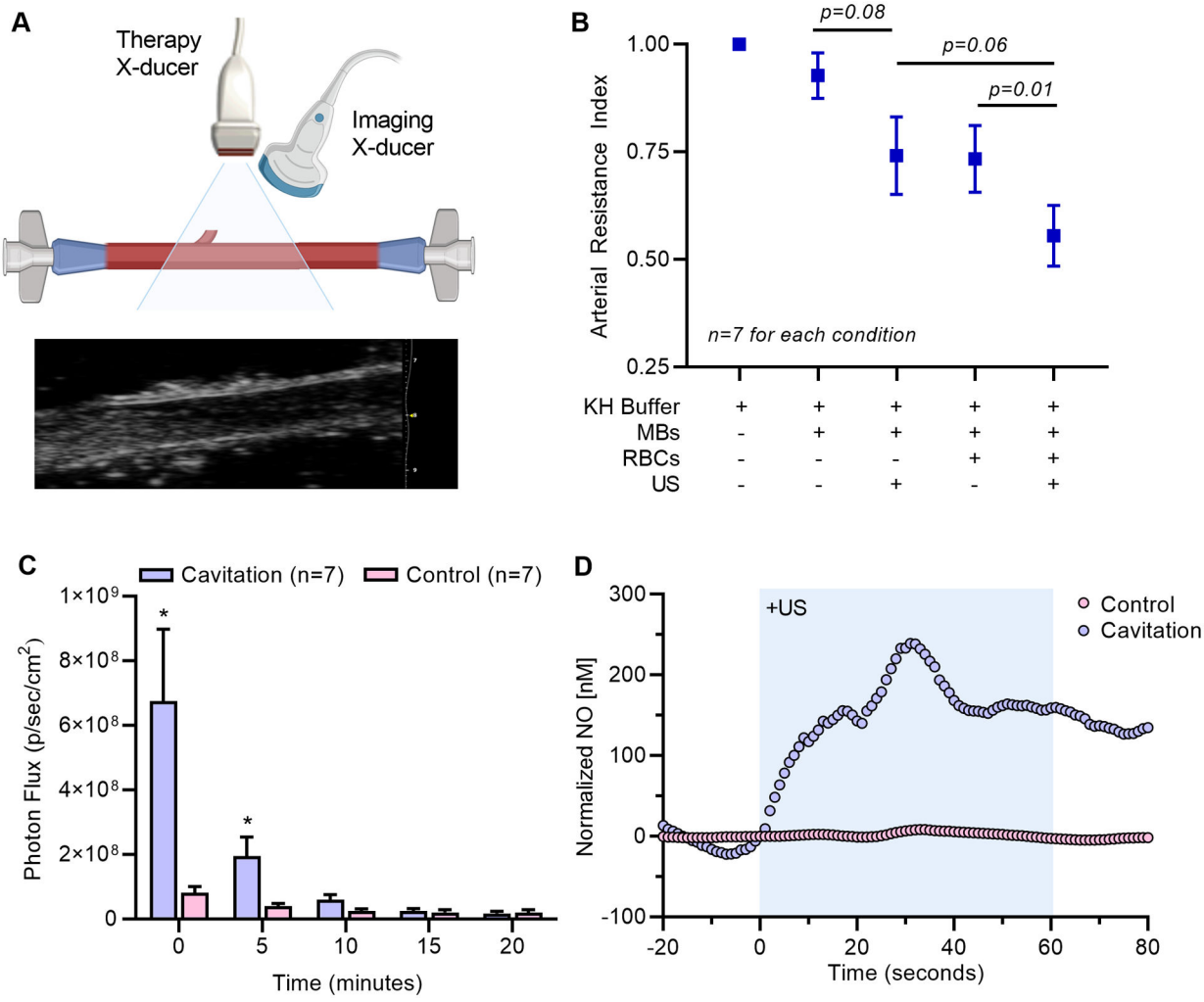

Figure 5.

(**A**) Illustration of the *ex vivo* perfused arterial preparation with simultaneous therapeutic ultrasound (*US*) for cavitation and high-frequency 2-D ultrasound imaging for arterial diameter. An example of the ultrasound imaging is shown. (**B**) Arterial resistance index (mean ±SEM) derived from diameter measurements for conditions with and without microbubbles (MB), US, and RBCs. Data are normalized to conditions with Krebs-Henseleit buffer (*KH*) alone. (**C**) Mean (±SEM) light activity from the derived from diameter measurements for conditions with and without microbubbles (MB), US, and RBCs. Data are normalized to conditions with Krebs-Henseleit buffer (*KH*) alone. (**C**) Photon flux (mean ±SEM) generated by the luminescent assay for extracellular ATP from *ex vivo* RBCs exposed to 1 min of cavitation and from time-matched control RBCs. Time 0 represents the first measurement which was approximately 45 seconds after cavitation. *p<0.05 vs control. Inset shows luminescence from cavitation and control experiments. (**D**) Example of real-time measurement of NO release in whole blood produced by ultrasound cavitation of MBs for 1 minute (shaded area). Data are normalized to the concentration at the time of US

initiation, and control experiments were performed by simultaneous measurement of RBCs not undergoing cavitation.

TABLE 1.

Vital Signs in Non-human Primates Undergoing Forearm Cavitation

	2-D Cavitation (n=5)			3-D Cavitation (n=6)		
	BL	**5 min**	**10 min**	**BL**	**5 min**	**10 min**
Heart Rate (min^{-1})	127±26	125±19	130±12	136±15	134±7	136±8
Systolic BP (mm Hg)	92±33	97±30	98±40	86±25	86±29	82±43
Diastolic BP (mm Hg)	42±14	44±27	43±18	46±18	39±12	48±22
O_2 Saturation (%)	98±2	98±3	98±3	97±3	98±3	97±3
Respiration (min^{-1})	27±1	32±4	34±2	27±3	30±7	31±7